International Journal on
"Technical and Physical Problems of Engineering"
(IJTPE)
Published by International Organization of IOTPE

ISSN 2077-3528
IJTPE Journal
www.iotpe.com
ijtpe@iotpe.com

March 2023 | Issue 54 | Volume 15 | Number 1 | Pages 45-51

EXPLORING THE IMPACT OF IMAGE ENHANCEMENT AND DATA AUGMENTATION TECHNIQUES ON LUNG DETECTION IN CHEST RADIOGRAPHY IMAGES

M.K. Jalehi B.M. Albaker

College of Engineering, Al-Iraqia University, Baghdad, Iraq, muhanned4mtd@gmail.com, baraamalbaker@ymail.com

Abstract- The health and wellbeing of people all over the world are being severely impacted by the ongoing COVID-19 pandemic. One of the most important ways to check for COVID-19 is chest radiography, so ensuring that infected people undergo this test is crucial. This research set out to assess the efficacy of various image enhancement and data augmentation techniques for use with digital chest X-Rays in the detection of COVID-19 patients. White-balance correction (WB) and contrast-limited adaptive histogram equalization (CLAHE) were the two methods used to improve the images. These two technologies have also been applied to examine this impact on COVID-19 discrimination. Also, Data was augmented in two distinct ways, using a different set of techniques and combining it with image enhancement techniques. Transfer learning was used to compare image classification models pre-trained on the ImageNet dataset to well-known deep learning architectures. Our models were evaluated and compared using the novel-combined chest X-Ray datasets. We observed that the VGG-16 model outperforms other models with an accuracy of 98% when image WB and CLAHE are used together. Due to their superior performance, these pre-trained models can greatly improve the speed and accuracy of COVID-19 diagnosis.

Keywords: Transfer Learning, Image Enhancement, COVID-19, X-Ray Dataset, White Balance, CLAHE, Data Augmentation.

1. INTRODUCTION

The coronavirus (COVID-19) outbreak is a global health concern. COVID-19 attacks the epithelial cells that line the inside of our lungs and causes muscle pain, an irritated throat, a symptom of a dry cough, pain in the head, and a high temperature [1]. Clinical evidence suggests that processing time for RT-PCR (reverse transcription polymerase chain reaction) (typically between 4 and 6 hours) and low positive rate in early infection stages are its main drawbacks [2], which is considered a long time given COVID-19 has a fast spread rate. As a result, tests using radiographs of the chest (CXR) and CT scans (CT) scans were recommended as another method than PCR testing and for its use as an early diagnostic tool [3]. Doctors frequently use CXRs' to diagnose illnesses like pneumonia, bronchitis, and emphysema.

Since CXR imaging equipment is standard in hospitals, it may be possible to test for COVID-19 using X-Rays rather than dedicated test kits. On the other hand, CXR images and CT scans present a significant challenge for radiologists, who must spend considerable time poring over each image and manually extracting relevant information. Furthermore, it's gotten more challenging for radiologists, particularly novices, due to the commonalities between contagious and inflammatory lung diseases and their shared patterns of progression, it can be challenging for individuals, to observe these subtle differences with the naked eye.

For radiologists to save time and come up with smarter solutions for diagnosing COVID-19, therefore, it is crucial that an efficient CAD system be developed quickly. Early detection of disease increases the likelihood that infected patients will respond favorably to treatment and decreases the likelihood that a transmissible illness like COVID-19 will spread throughout the community. Doctors frequently use X-Ray images to diagnose lung diseases. X-Rays, CT scans, and other medical imaging technologies play a key role in COVID-19 testing [4].

Radiologists manually analyze these pictures to look for some visible signs of infection. These visual markers can be used as an alternative to traditional methods for quickly identifying patients who are impacted. Most healthcare systems can use CXR imaging instead of CT, which call for pricey machinery and regular upkeep. With the CXR system, examinations can be done safely within an isolation room, decreasing the likelihood of spreading COVID-19, which is impossible with fixed CT scanners. CXR also allows for quick triage of suspected COVID-19 cases. As a result, CXR images are used in this study to diagnose COVID-19 automatically.

Because COVID-19 infections are most commonly found in the lungs, chest radiographs (chest X-Rays or CT scans) have been routinely used [5], radiologists manually analyze these pictures to look for some visible signs of infection. These visual markers can be used as an alternative to traditional methods for quickly identifying patients who are impacted.

While CT scans produce more detailed images, chest X-Ray images are more easily movable and handy, and provide faster triage. Convolutional neural networks (CNNs) are particularly used for extracting relevant features from images, making them a powerful tool for extracting features from medical images [6]. In this paper, the effect of performing image enhancement and data augmentation operations in the deep convolutional neural network is evaluated and compared to see how it affects the diagnosis of COVID-19.

2. RELATED WORKS

Many researchers have used artificial intelligence techniques to improve AI's performance in the face of the COVID-19 pandemic. Gupta, et al. propose the InstaCovNet-19 model. It achieves 99% accuracy in detecting COVID-19 and pneumonia by stacking (Xception, ResNet101, MobileNetV2, NASNet, and InceptionV3) models [7]. To detect COVID-19, Using 2362 CXR images from four hospitals, Goldstein, et al. [8] trained a pre-trained ResNet50 model with the help of data augmentation and lung segmentation, resulting in an accuracy of 89.7% and a sensitivity of 87.1%. The LungCov methodology was proposed for diagnosing COVID-19 by S. Kumar and H. Kumar [9]. Their work is primarily focused on enhancing the care that is provided by the healthcare system as well as the services it provides to society. For use in assisting radiologists in the diagnosis of coronavirus from X-rays images, Hemdan, et al. [10] design the COVIDXNet model.

A number of models, including InceptionV3, MobileNetV2, VGG19, DenseNet201, ResNetV2, and Xception, were compared, which are all pretrained DL networks. The VGG model performed at a 90% accuracy level in their experiments. Converging Convolutional Neural Networks for Feature Extraction with SVM Classification, Sethy and Behera [11] proposed a hybrid technique for diagnosing COVID-19-infected patients using CXR images. Antin B, Kravitz J, and Martayan E [12], suggested a differential classification approach in which X-ray chest images are used as inputs and the outputs are either pneumonia or non-pneumonia in both classes. Using the VGG16, VGG19, and MobileNet neural networks, H. Moujahid, et al. [13] develop a DL-CNN-based strategy to analyze coronavirus infections and differentiate them from other types of pneumonia and healthy; this is essential due to the scarcity of high-quality X-Ray image databases for coronavirus patients. They use Grad-CAM to visually interpret the results.

Our paper follows the structure described below: Section 3, present a theoretical information on (3.1) techniques for improving images, and (3.2) demonstrates the effect of the data augmentation techniques used in this paper. Section 4 covers the materials and methods for (4.1) dataset details and (4.2) data preprocessing. In Section 5, the demonstrate of (5.1) the models' evaluation, (5.2) the obtained results and analysis, and (5.3) the evaluation against current best practices. Section 6 has a discussion, section 7: Closing remarks and future works.

3. BACKGROUND

3.1. Image Enhancement Techniques

Image enhancement is a useful technique in the field of image processing because it can improve the quality of an image with poor resolution, blurry edges, or low contrast, and then extract useful information from that image. In this study, two types of enhancement techniques are employed and a hybrid of the two that we refer to as (imgE). These techniques are:

- The white-balance (WB) algorithm is an imaging processing technique that is used to adjust a digital image's color fidelity. By stretching RGB channels independently, colors in the image's visible layers are tweaked by the white-balance algorithm. The end pixels of the three channels are thrown away because they're only used by 0.05% of the image's total pixels. This adjustment eliminated the potential for the pixel colors near the channel's end to have a negative effect on the range of allowed values when stretching [14]. The White Balance Algorithm can be found at [15].
- Contrast limited adaptive histogram equalization (CLAHE) is a useful contrast enhancement technique that effectively helps to increase the image's contrast. CLAHE is a new and enhanced form of the adaptive histogram equation (AHE). Figure 1 show an example of image enhancement work. CLAHE was useful in examining various medical images in previous research. It was found to be helpful in improving a wide variety of medical images and produced outstanding results in enhancing chest CT scans. CLAHE is calculated as described in [16]. An example of image enhancement work is shown in Figure 1.

3.2. Data Augmentation

In the training of deep neural networks, data augmentation is commonly used. Many state-of-the-art as a key component. Today's deep neural networks have billions of parameters, leading to overfitting on small amounts of training data. The goal of data augmentation is to enrich training data by adding to it and making it more diverse, decreasing overfitting and enhancing generalization [17].

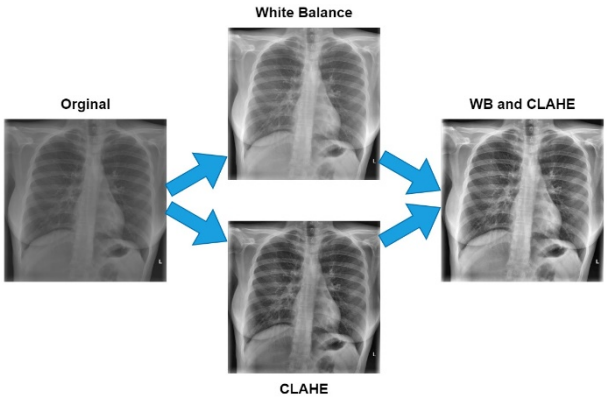

Figure 1. Images have been already processed with white balance and CLAHE applied

4. MATERIALS AND METHODS

4.1. Dataset

A new combination dataset was proposed where the x-ray images from seven publicly available datasets were combined into one dataset with a total of 6,136 X-ray images. Table 1 presents the reference and number of images in each dataset. After that, the repeated images were removed, and make sure that all image extensions are allowed to work in the CNN models by converting all images to PNG. At last, the dataset was divided into three equal parts, with 60% going to training, 20% to validation, and 20% to testing. Each class was divided into two classes: COVID-19 and NORMAL, each of which had 3,068 images.

Table 1. Dataset information

References	Contents	Image distribution	
COVID-CXNet [18]	The SIRM database is used for chest x-ray images of patients who tested positive for COVID-19 via polymerase chain reaction.	COVID-19	839
COVID-chestxray dataset [19]	COVID-19, Pneumonia, Pneumocystis, Streptococcus, No Finding, E.Coli, Klebsiella, Legionella, SARS, Lipoid, Varicella, Mycoplasma, Influenza, Tuberculosis.	COVID-19	57
Chest X-ray (COVID-19 and Pneumonia) [20]	The dataset consists of two main directories (train and test) with three subdirectories each (COVID19, PNEUMONIA, NORMAL). Total images: 6,432	Normal	1,583
		COVID-19	576
		Pneumonia	4,273
COVID CXR Image Dataset (Research) [21]	Posteroanterior (PA) chest X-ray images of normal, viral, and COVID-19-affected patients are included in this dataset. Total images: 1,823	Normal	668
		COVID-19	536
		Virus	619
COVID-19 X-ray - Two proposed Datasets [22]	In this dataset consists Five classes COVID-19, Bacterial Pneumonia, Viral Pneumonia, Lung Opacity No Pneumonia, Normal. Total images: 5,688	Normal	711
		COVID-19	711
COVID19 Pneumonia Normal Chest Xray (PA) Dataset [23]	The dataset is organized into 3 folders (Covid19, pneumonia, normal) which contain chest X-ray posteroanterior (PA) images. Total images: 4,525	Normal	1,525
		COVID-19	1,525
Curated Chest X-Ray Image Dataset for COVID-19 [24]	This is a combined curated dataset of COVID19 Chest X-ray images obtained by collating 15 publicly available datasets. Total images: 9,208	Normal	3,270
		COVID-19	1,281
Cx7 dataset	Merging seven datasets while keeping the COVID-19 and Normal classes in equilibrium. Total images: 6136	Normal	3,068
		COVID-19	3,068

4.2. Data Preprocessing

X-ray images come in repositories and on Kaggle in various formats and sizes, ranging from 224×224 to 5623×4757 pixels. Each image in the datasets was first resized to 320 by 320 pixels, keeping the aspect ratio (these dimensions were chosen to be used on all models). From the final dataset, three datasets were produced (white balance, CLAHE, and imgE), respectively, for evaluating the models' performance. After that, Inside the models, all images were resized to 224×224 px except the InceptionResNetV2 model, where images were resized to 299×299 px. to meet the model's requirements, Keras "preprocess input" function normalizing/centering all resized images. The results of applying the eight pre-trained models to the original dataset (before any image enhancement or augmentation) are shown in Table 2. The transfer learning process of this research used the VGG-16, ResNet50V2, DensNet121, InceptionResNetV2, MobileNetV2, MobileNetV3, and EfficientNetB0 networks, with the weights pretrained on the ImageNet dataset. This work trains the models with a 32-batch size and 100 epochs as the max threshold.

The GlobalAveragePooling2D layer was placed on top of the CONV-base, which applies average pooling to the spatial dimensions until each is one but leaves the other dimensions alone [25]. The AVG POOL function's output was piped to two fully connected layers, each of which was followed by a dropout layer with a 0.2 rate. The output layer is used for the final classification in the last layer. If the output of the "preprocess input" function is [0-1], then we use the sigmoid activation function, and if [-1, 1], then we use from_logits=True. Furthermore, Adam optimizer and BinaryCrossentropy for loss function were used. After that, to improve the model training and prevent overfitting, callback functions are used, such as ModelCheckpoint, EarlyStopping for patience=11, and ReduceLROnPlateau for patience=2 and factor=0.2.

Table 2. Results of Applying Seven pre-Trained Models

Models	Accuracy	Precision	Sensitivity
VGG-16	97.71%	98.5%	96.9%
VGG-19	96.9%	96.9%	96.9%
DenseNet201	96.25%	96.24%	96.24%
ResNet50V2	97.14%	97.2%	97%
InceptionResNetV2	96%	96%	96%
EfficientNetB0	97%	97%	97%
MobileNetV2	97.63%	97.71%	97.55%
MobileNetV3	97.55%	97.55%	97.55%

Table 3. Result of seven pre-trained models after applying image enhancement

Models	WB/ CLAHE	Accuracy	Precision	Sensitivity
VGG-16	imgE	98%	98.35%	97.71%
VGG-19	WB	97.22%	97.22%	97.22%
DenseNet201	imgE	96.16%	96.24%	96%
ResNet50V2	imgE	96.9%	96.9%	96.9%
InceptionResNetV2	WB	96%	96%	95.92%
EfficientNetB0	imgE	97.71%	97.71%	97.71%
MobileNetV2	WB	97.63%	97.55%	96.71%
MobileNetV3	WB	97.63%	97.71%	97.55%

The general schematic of the transfer learning process used in the models is shown in Figure 2. The best performance results for each model when applying white balance, CLAHE, or a combination of WB and CLAHE (imgE) are shown in Table 3. Offline augmentation means performing the augmentation operations before making the model and saving the augmented images on the hard disk. While online data augmentation means performing augment operations while the model is working, i.e., loading images into memory to perform operations on them. Different techniques were used to analyze the performance based on the MobileNetV3 model, such as the imgAug library and Keras layers. While Table 4 shows the implementation results of these techniques.

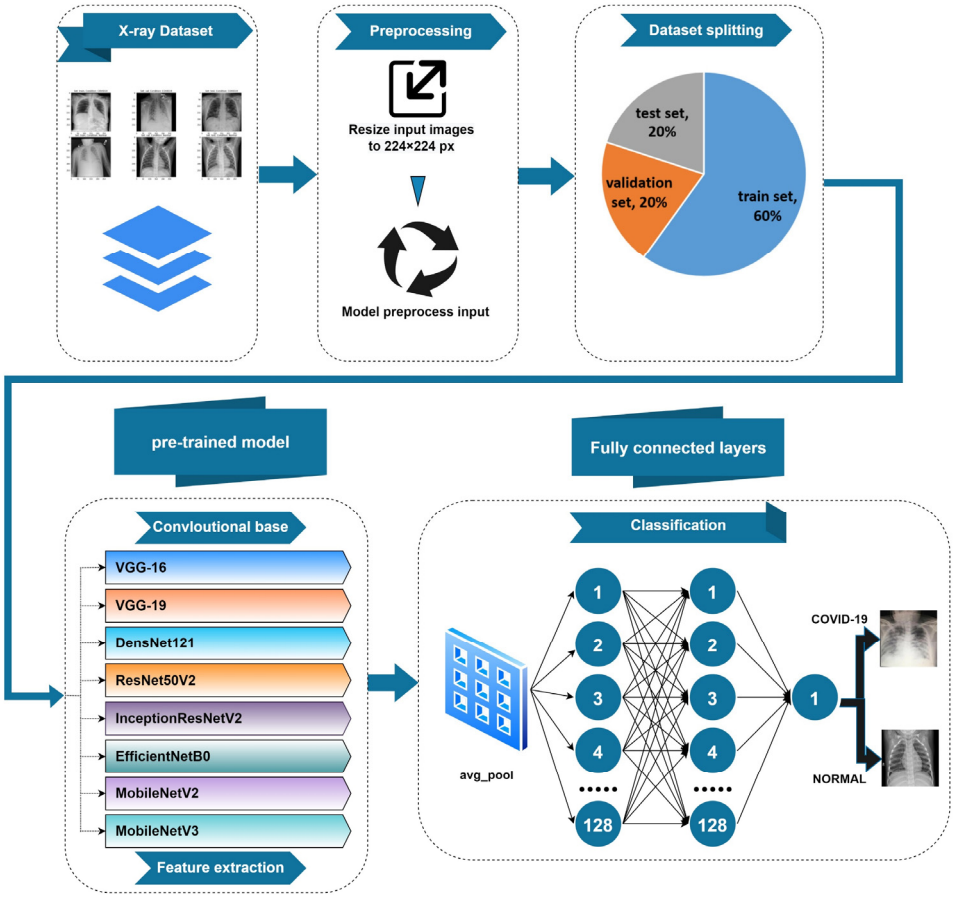

Figure 2. The proposed CNN model's block diagram process

Table 4. Result of online and offline data augmentation techniques

Augmentation technique		Augmentation type	Acc. %	Precision %	Sensitivity %
offline	imgAug	Rotation + trans + zoom + crop	95.2	94.83	95.6
Online	Keras Layers	Rotation	95.27	95.26	95.26
		Rotation + RandomContrast	96.41	96.26	96.57
		Rotation + trans + zoom + contrast	92	92	92
	Simple imgAug	images are cropped, affinely transformed, some are flipped horizontally, noise and blur are added, and the contrast and brightness are adjusted	91.19	90.52	92
	Heavy imgAug	a long series of augmenters that causes substantial alterations to the augmented images	91.19	90.52	92

The values of the augmentation techniques that were used in the models are: Keras layer: RandomRotation=0.2, RandomTranslation=(0.1,0.1), Random-Zoom= (0.1,0.1). In the imgaug library we used the values as they are in the library. The results of the combination of data augmentation and image enhancement techniques are shown in Table 5, where data augmentation was applied with white balance, CLAHE, or both of them (imgE).

Table 5. Result of seven pre-trained models after combining (DA and Image enhancement) techniques

Models	DA/WB/ imgE	Acc. %	Precision %	Sensitivity %
VGG-16	DA, WB	97.47	97.39	97.55
VGG-19	DA, WB	95.9	95.9	95.9
DensNet201	DA, imgE	95.76	95.75	95.75
ResNet50V2	DA, WB	97	97	97
InceptionResNetV2	DA, WB	94.62	94.47	94.77
EfficientNetB0	DA, imgE	97.14	97.22	97
MobileNetV2	DA, WB	96.65	96.73	96.57
MobileNetV3	DA, imgE	96.33	96.25	96.41

5. EVALUATION AND RESULTS

5.1. Performance and Evaluation Metrics

Accuracy (Acc) and precision (Pre), also known as positive prediction value and negative prediction value, are the most popular metrics used for evaluating models. Sensitivity (Sen) or probability of detection. There are four primary metrics used in the computation of these measures: true positives, which are cases of a disease that were successfully diagnosed (TP), true negatives (healthy cases), were successfully identified (TN), disease cases not being properly identified as having the disease (FN), and inaccuracies in the diagnosis of healthy people (false positives) (FP). The formulas required to determine the accuracy, precision, and sensitivity of measurements is provided as in [26].

5.2. Results

The evaluation of the effectiveness of data augmentation and image enhancement techniques is based on metrics results obtained by conducting experiments with pretrained CNN models. On the other hand, the test set was used to verify the model's performance and contained samples not included during the training phase. Table 2 lists the details of the result of applying eight pre-trained models without the implementation of data augmentation or image enhancement techniques. The VGG-16 model has higher accuracy. The effect of image enhancement techniques (white balance and CLAHE), with the effect of combining them (imgE), has been tested on the eight models, as shown in Table 3. The results shows that the VGG16 has the highest rating by using imgE. Also, it shows that all models' accuracy increased, except for the Dense-Net121 model, which decreased slightly, and the InceptionResNetV2 model remained the same. Table 4 shows the test results of data augmentation techniques. Table 4 shows utilization of data augmentation techniques for offline and online augmentation.

The results show an increase in the accuracy in the case of online augmentation using the Keras Layers when using Rotation with RandomContrast. The results produced from the combination of data augmentation and image enhancement techniques are shown in Table 5. The results show a decrease in accuracy for all models except for ResNet50V2, where its accuracy increased. In a summary, the models VGG-16, MobileNetV2, MobileNetV3, and EfficientNetB0 provide the best predictive performance. Whereas the EfficientNetB0 model offers the best predictive balance. The VGG16 model showed the highest performance during the experiments. A confusion matrix is a performance calculation used in deep learning to solve classification problems, as depicted in Figure 3.

5.3. Comparison with State-of-the-Art Methods

Table 6 compares our top model for detecting COVID-19 in chest X-Rays to other cutting-edge deep learning techniques. Each of the table's methods has been reimplemented using our Cx7 dataset to classify COVID-19 and normal X-Rays. The obtained results showed that our proposed model performed better than the latest methods in the table in terms of accuracy for the two-class classification task (98%).

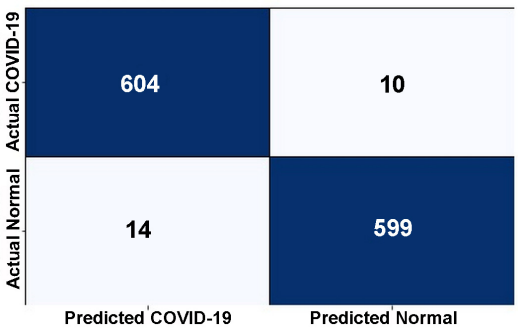

Figure 3. Illustrates the VGG16 model performance with the imgE technique with the confusion matrix that goes with it

It also has the potential to greatly assist radiologists in avoiding hospital and medical system overcrowding. With an accuracy of 98% our proposed model successfully classifies COVID-19, making it useful for radiologists in the diagnosis of COVID-19.

Table 6. Comparison of results with other existing state-of-the-art methods

Method/ Model	Acc.	Precision	Sensitivity
Transfer learning (VGG-16) [26]	95.51%	92.79%	98.69%
Transfer learning (Xception) [27]	91.93%	89.9%	94.45%
Training from scratch based on VGG-19 architecture [13]	95.11%	95.10%	95.10%
Training from scratch (Scenario-3) [28]	85.17%	84.39%	86.31%
Proposed model (VGG-16)	98%	98.35%	97.71%

6. DISCUSSION

The number of epochs, data augmentation, image enhancement techniques, imaging methods, image content, image quantity, dataset distribution, model structure, model complexity, loss function, optimizer, and other factors all influence the performance of a single model. According to the results, when image enhancement and data augmentation techniques are used, the accuracy improves in some models while it worsens in others. While the accuracy of models (VGG19, InceptionResNetV2, MobileNetV2, MobileNetV3) improved when using white balance technology, the accuracy of models (VGG16, Dense-Net201, ResNet50V2, EfficientNetB0) improved when applying CLAHE technology.

On the other hand, several techniques were tested for data augmentation based on the MobileNetV3 model for its speed in training. The best method was Keras layers to augment the data using (Rotation with RandomContrast) techniques. In this study, the proposed model was applied to the Cx7 dataset and showed real and promising accuracy in classifying COVID-19 utilizing CXR images. When the images were improved using the white balance technique, the VGG16 model outperformed the other models, with an accuracy of 98%. As a result, this model was chosen to compare with state-of-the-art models in other related works.

7. CONCLUSIONS AND FUTURE WORK

As a significant contribution, a compiled 6136 images from three publicly available X-Ray datasets and divided them into two categories: The benchmark dataset will consist of 3068 coronavirus-infected lungs and 3068 healthy lungs and will be made publicly available. Furthermore, using deep convolutional neural networks, different image quality improvement methods were evaluated for detecting coronavirus in CXR images automatically.

In addition, several types of data augmentation techniques were tested and compared. The next step is to use chest X-Ray images to look for and identify coronaviruses, the performances of eight CNN models with various deep neural network models were compared. With a combination of white balance and CLAHE techniques, our best-performing VGG-16 achieved an

accuracy of 98% on the test set. Several dimensions will be addressed in future work to widen the search in datasets, including compiling more X-Ray images, especially from local hospitals, to enhance the accuracy. This deep AI-based approach has the potential to be used as a rapid diagnostic instrument to save person's life or reduce deaths, especially throughout pandemics when delays or misdiagnoses can have devastating consequences.

REFERENCES

[1] F. Wu, et al., "A New Coronavirus Associated with Human Respiratory Disease in China", Nature, Vol. 579, No. 7798, pp. 265-269, February 2020.

[2] D.K.W. Chu, et al., "Molecular Diagnosis of a Novel Coronavirus (2019-nCoV) Causing an Outbreak of Pneumonia", Clin Chem, Vol. 66, No. 4, pp. 549-555, April 2020.

[3] S. Hassantabar, et al., "CovidDeep: SARS-CoV-2/COVID-19 Test Based on Wearable Medical Sensors and Efficient Neural Networks", IEEE Transactions on Consumer Electronics, Vol. 67, No. 4, pp. 244-256, November 2021.

[4] F. Shi, et al., "Review of Artificial Intelligence Techniques in Imaging Data Acquisition, Segmentation, and Diagnosis for COVID-19", IEEE Reviews in Biomedical Engineering, Vol. 14, pp. 4-15, 2021.

[5] M. Chung, et al., "CT imaging Features of 2019 Novel Coronavirus (2019-NCoV)", Radiology, Vol. 295, No. 1, pp. 202-207, February 2020.

[6] E.H. Hssayni, M. Ettaouil, "Generalization Ability Augmentation and Regularization of Deep Convolutional Neural Networks Using $l^{1/2}$ Pooling", International Journal on Technical and Physical Problems of Engineering (IJTPE), Issue 48, Vol. 13, No. 3, pp. 1-6, September 2021.

[7] A. Gupta, Anjum, S. Gupta, R. Katarya, "InstaCovNet-19: A Deep Learning Classification Model for the Detection of COVID-19 Patients Using Chest X-Ray", Applied Soft Computing, Vol. 99, p. 106859, February 2021.

[8] D. Keidar, et al., "COVID-19 Classification of X-Ray Images Using Deep Neural Network", European Radiology, Vol. 31, No. 12, pp. 9654-9663, December 2021.

[9] S. Kumar, H. Kumar, "LungCov: A Diagnostic Framework Using Machine Learning and Imaging Modality", International Journal on Technical and Physical Problems of Engineering (IJTPE), Issue 51, Vol. 14, No. 2, pp. 190-199, June 2022.

[10] E.E.D. Hemdan, M.A. Shouman, M.E. Karar, "COVIDX-Net: A Framework of Deep Learning Classifiers to Diagnose COVID-19 in X-Ray Images", arxiv, March 2020, https://arxiv.org/abs/2003.11055v1.

[11] P. Kumar Sethy, S. Kumari Behera, P. Kumar Ratha, P. Biswas, "Detection of Coronavirus Disease (COVID-19) Based on Deep Features and Support Vector Machine", PrePrints, 2020, www.preprints.org.

[12] B. Antin, J. Kravitz, E. Martayan, "Detecting Pneumonia in Chest X-Rays with Supervised Learning", SemanticScholar, 2017.

[13] H. Moujahid, et al., "Combining CNN and Grad-Cam for Covid-19 Disease Prediction and Visual Explanation", Intelligent Automation and Soft Computing, Vol. 32, No. 2, pp. 723-745, 2022.

[14] "8.17. White Balance", February 2022, https://docs. gimp.org/2.10/en/gimp-layer-white-balance.html.

[15] "White Balance Algorithm", February 2022, https:// adadevelopment.github.io/gdal/white-balance-gdal.html.

[16] J.B. Zimmerman, S.M. Pizer, E.V. Staab, J.R. Perry, W. Mccartney, B.C. Brenton, "An Evaluation of the Effectiveness of Adaptive Histogram Equalization for Contrast Enhancement", IEEE Transactions on Medical Imaging, Vol. 7, No. 4, pp. 304-312, 1988.

[17] Z. Tang, Y. Gao, L. Karlinsky, P. Sattigeri, R. Feris, D. Metaxas, "Online Augment: Online Data Augmentation with Less Domain Knowledge", Lecture Notes in Computer Science (Including Subseries Lecture Notes in Artificial Intelligence and Lecture Notes in Bioinformatics), Vol. 12352 LNCS, pp. 313-329, August 2020.

[18] A. Haghanifar, M.M. Majdabadi, Y. Choi, S. Deivalakshmi, S. Ko, "COVID-CXNet: Detecting COVID-19 in Frontal Chest X-ray Images Using Deep Learning", arxiv, Version 2, June 2020, https://arxiv.org/abs/2006.13807v2.

[19] J.P. Cohen, P. Morrison, L. Dao, K. Roth, T.Q. Duong, M. Ghassemi, "COVID-19 Image Data Collection: Prospective Predictions Are the Future", arxiv, Version 1, June 2020, http://arxiv.org/abs/2006.11988.

[20] Prashant Patel, "Chest X-ray (Covid-19 and Pneumonia)", Kaggle, https://www.kaggle.com/datasets/ Prashant.
268/chest-xray-covid19-pneumonia, February 2022.

[21] J.P. Cohen, P. Morrison, L. Dao, "COVID-19 Image Data Collection", arxiv, Version 1, March 2020, http://arxiv.org/abs/2003.11597.

[22] E. Vantaggiato, E. Paladini, F. Bougourzi, C. Distante, A. Hadid, and A. Taleb-Ahmed, "Covid-19 Recognition Using Ensemble-CNNS in Two New Chest X-Ray Databases", Sensors, Vol. 21, No. 5, pp. 1-20, March 2021.

[23] Amanullah Asraf, "COVID19 Pneumonia Normal Chest Xray (PA) Dataset", Kaggle, November 2021. www.kaggle.com/amanullahasraf/covid19-pneumonia-normal-chest-xraypa-dataset?select=COVID19_ Pneumonia_Normal_Chest_Xray_PA_Dataset.

[24] Unais Sait, "Curated Chest X-Ray Image Dataset for COVID-19", Kaggle, November 2021, www.kaggle.com/ unaissait/curated-chest-xray-image-dataset-for-covid19.

[25] M. Lin, Q. Chen, S. Yan, "Network in Network", The 2nd International Conference on Learning Representations, ICLR 2014, March 2014. https://arxiv.org/abs/1312.4400v3.

[26] T. Fawcett, "An Introduction to ROC Analysis", Pattern Recognit Lett, Vol. 27, No. 8, pp. 861-874, June 2006.

[27] M.D.K. Hasan, et al., "Deep Learning Approaches for Detecting Pneumonia in COVID-19 Patients by Analyzing Chest X-Ray Images", Mathematical Problems in Engineering, Vol. 2021, 2021.
[28] R. Jain, M. Gupta, S. Taneja, D.J. Hemanth, "Deep Learning-Based Detection and Analysis of COVID-19 on Chest X-Ray Images", Applied Intelligence, Vol. 51, No. 3, pp. 1690-1700, March 2021.
[29] M. Loey, S. El Sappagh, S. Mirjalili, "Bayesian-Based Optimized Deep Learning Model to Detect COVID-19 Patients Using Chest X-ray Image Data", Computers in Biology and Medicine, Vol. 142, p. 105213, March 2022.

BIOGRAPHIES

Name: **Muhannad**
Middle Name: **Kassem**
Surname: **Jalehi**
Birthday: 01.01.1988
Birth Place: Baghdad, Iraq
Bachelor: Computer Technology Engineering, Department of Computer Technology Engineering, Al-Rafidain University College, Baghdad, Iraq, 2019
Master: Student, Computer Engineering, Department of Computer Engineering, Faculty of Engineering, Al-Iraqia University, Baghdad, Iraq, Since 2022
Research Interests: Artificial Intelligence, Image Processing, Images Classification
Scientific Publications: 2 Papers, 1 Thesis
Scientific Memberships: Iraqi Engineers Association

Name: **Baraa**
Middle Name: **Munqith**
Surname: **Albaker**
Birthday: 29.01.1978
Birth Place: Baghdad, Iraq
Bachelor: Electrical Engineering, Department of Electrical Engineering, Faculty of Engineering, University of Baghdad, Baghdad, Iraq, 2000
Master: Electrical Engineering, Department of Electrical Engineering, Faculty of Engineering, University of Baghdad, Baghdad, Iraq, 2003
Doctorate: Control Systems, Department of Electrical Engineering, Faculty of Engineering, University of Malaya, Kuala Lumpur, Malaysia, 2012
The Last Scientific Position: Assist. Prof., Head of Electrical Engineering Department, Faculty of Engineering, Al-Iraqia University, Baghdad, Iraq, Since 2019
Research Interests: Contemporary Development in Computer and Control Applications
Scientific Publications: 30 Papers, 2 Book Chapters
Scientific Memberships: Iraqi Engineers Association